

Supporting Information

Mn₃O₄ Nanoparticles on Layer-Structured Ti₃C₂ MXene towards Oxygen Reduction Reaction and Zinc-air Battery

*Qi Xue, Zengxia Pei, Yan Huang, Minshen Zhu, Zijie Tang, Hongfei Li, Yang Huang, Na Li, Haiyan Zhang and Chunyi Zhi**

Preparation of Ti₃C₂ MXene

Ti₃AlC₂ (1 g) powder was immersed in 10 mL 48% HF, and stirred for 20 h at room temperature. The obtained powder was then rinsed multiple times with deionized water. The powder pellet was retrieved by centrifugation at 3500 rpm for 10 min, and the supernatant was discarded. The final product (Ti₃C₂T_x powder) was dried at 80 °C under vacuum for 12 h.

The mass/atomic ratio between Mn₃O₄ and MXene (Mn₃O₄ and AB) were calculated according to synthesis method. The mass ratio between Mn₃O₄ and MXene is about 30.5/10, the mass ratio between Mn₃O₄ and AB is about 30.5/10. In addition, atomic ratio between Mn₃O₄ and MXene is about 20/9. Since the AB is composed of carbon atoms, the atomic ratio between Mn₃O₄ and AB is around 12/75.

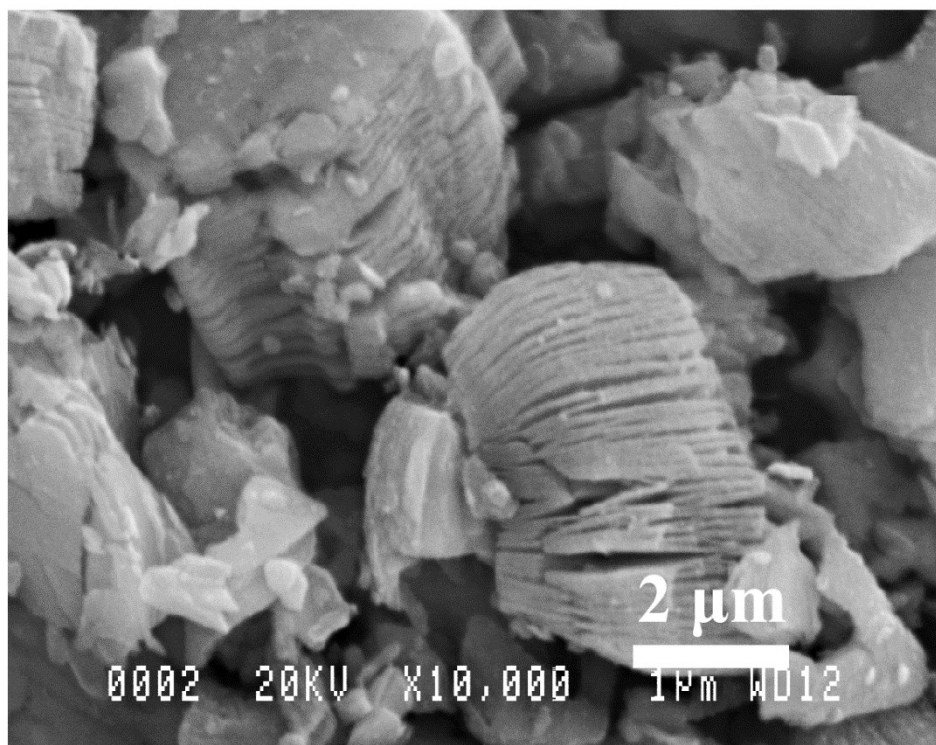


Fig. S1 SEM image of as-synthesized layered Ti_3C_2 MXene.

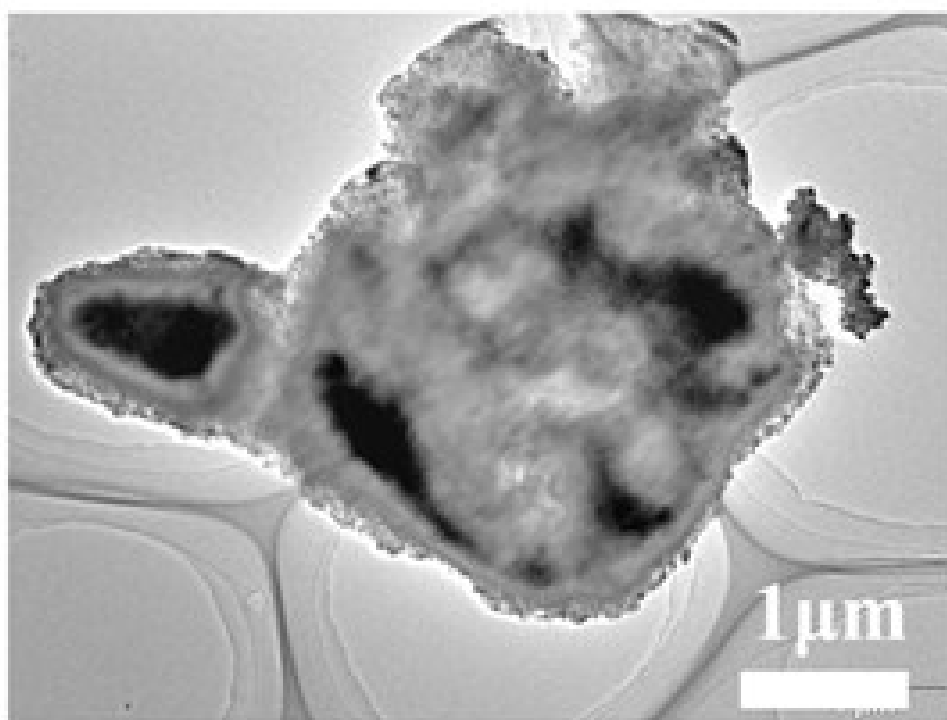


Fig. S2 TEM image of $\text{Mn}_3\text{O}_4/\text{MXene}$ nanocomposite under low resolution.

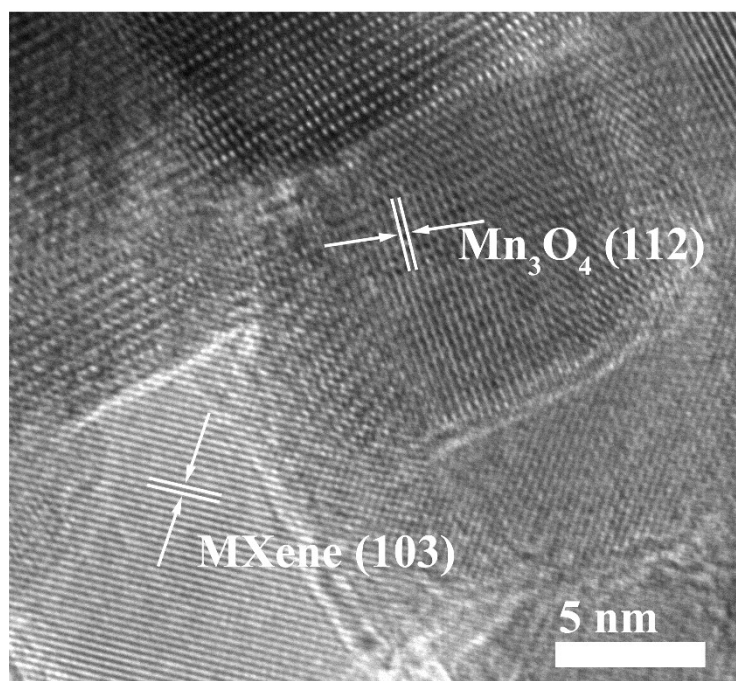


Fig. S3 HRTEM image of Mn₃O₄/MXene nanocomposite.

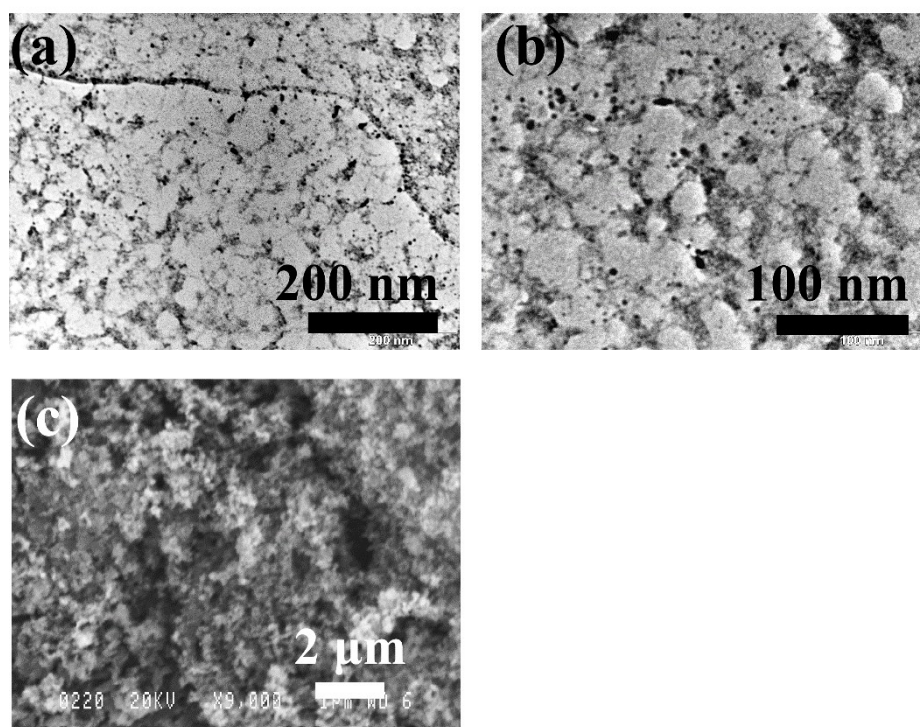


Fig. S4(a) and (b) TEM images of Mn₃O₄/AB nanocomposite. (c) SEM image of Mn₃O₄/AB nanocomposite.

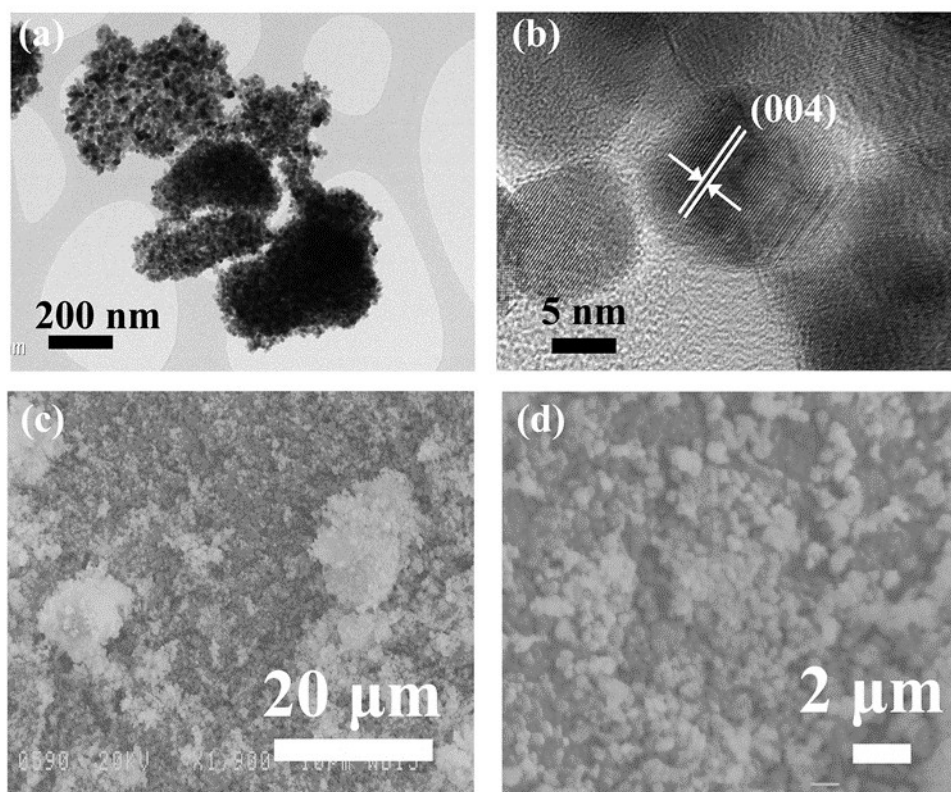


Fig. S5 TEM image (a) and HRTEM image (b) of Mn_3O_4 nanoparticles. (c) and (d) SEM images of Mn_3O_4 nanoparticles.

The synthesis method of Mn_3O_4 nanoparticles is same as the synthesis of $\text{Mn}_3\text{O}_4/\text{MXene}$ without adding of MXene. Lattice fringes with an inner-plane spacing at 0.234 nm displayed in HRTEM image of Mn_3O_4 nanoparticles, which can be attributed to (004) planes of hausmannite (Fig. S4b).^[1] The morphology of Mn_3O_4 nanoparticles depicted in Fig. S4c and Fig.S4d is in consistent with the morphology of Mn_3O_4 nanoparticles in Fig. 2a and Fig. 2b.

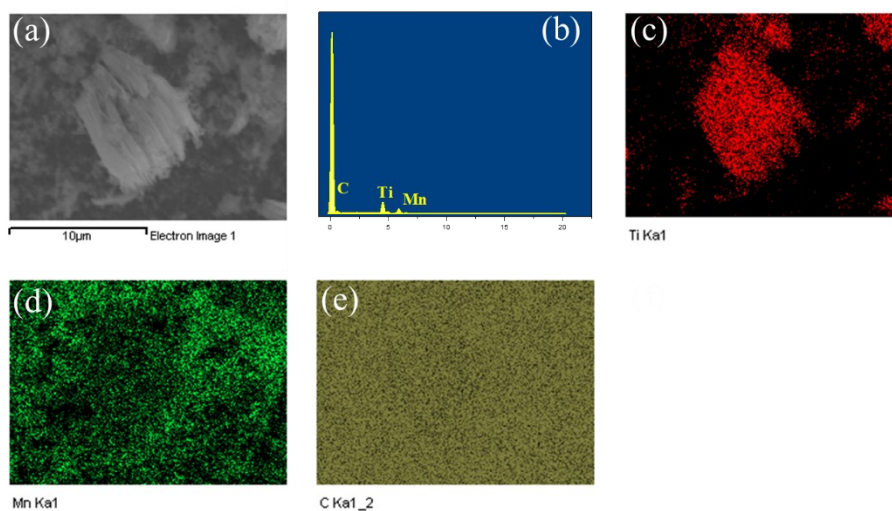


Fig. S6 (a) SEM image of Mn₃O₄/MXene. (b) Element composition of Mn₃O₄/MXene. (c) Element mapping images of Ti. (d) Element mapping images of Mn. (e) Element mapping images of C.

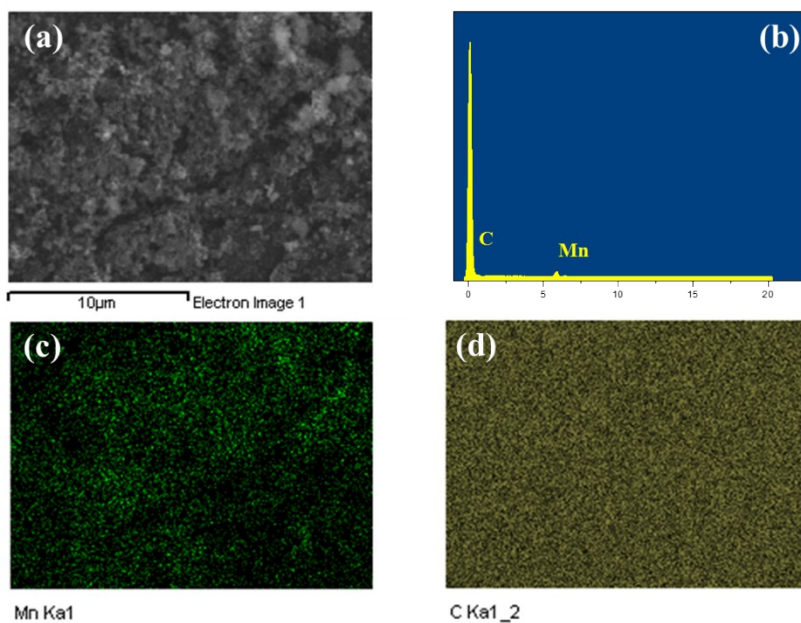


Fig. S7 (a) SEM image of Mn₃O₄/AB. (b) Element composition of Mn₃O₄/AB. (c) Element mapping images of Mn. (d) Element mapping images of Mn.

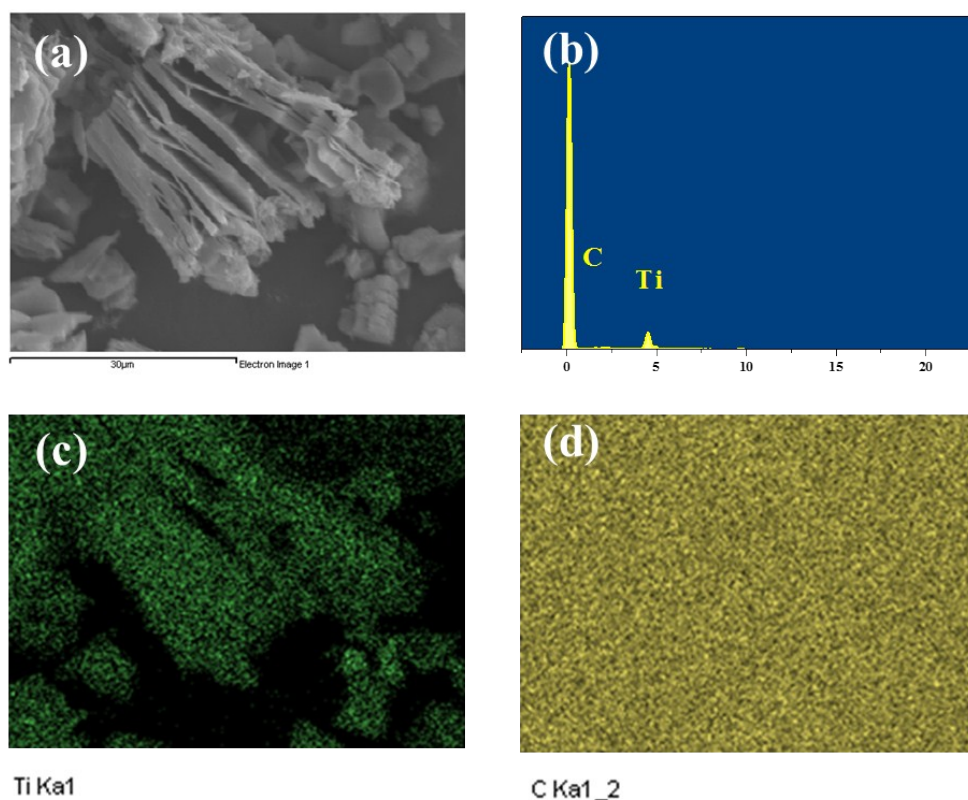


Fig. S8 (a) SEM image of layered Ti_3C_2 MXene in control experiment. (b) Element composition of corresponding Ti_3C_2 MXene. Element mapping images of Ti (c) and C (d) of corresponding Ti_3C_2 MXene.

As exhibited in Fig. S7, the Ti_3C_2 MXene in control experiment still retain the layered structure of MXene owing to the mild reaction condition.^[2]

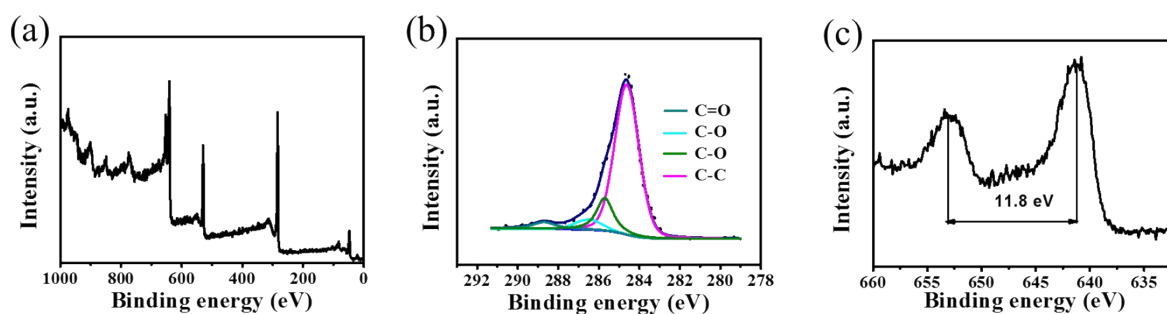


Fig. S9 XPS spectra of AB with Mn_3O_4 nanoparticles. (a) Full spectra. (b) High-resolution $\text{C}1\text{s}$ spectrum. (c) High-resolution $\text{Mn}2\text{p}$ spectrum.

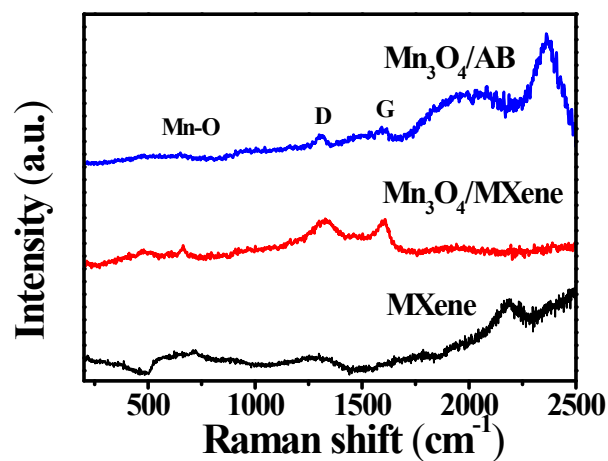


Fig. S10 Raman spectra of $\text{Mn}_3\text{O}_4/\text{AB}$, $\text{Mn}_3\text{O}_4/\text{MXene}$, and MXene.

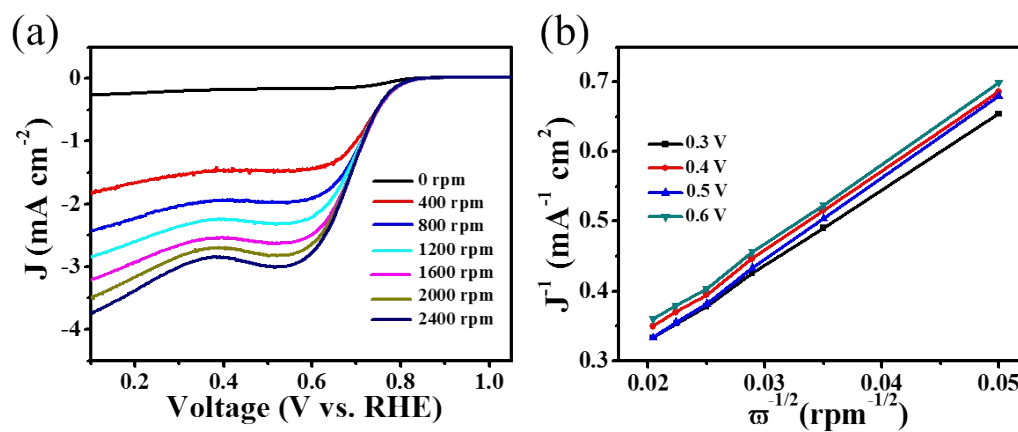


Fig. S11 (a) LSV curves of $\text{Mn}_3\text{O}_4/\text{AB}$ at different rotating speed with a sweep rate of 5 mV/s. (b) Calculated K–L plots of $\text{Mn}_3\text{O}_4/\text{AB}$. Catalyst loading was 0.1 mg/cm².

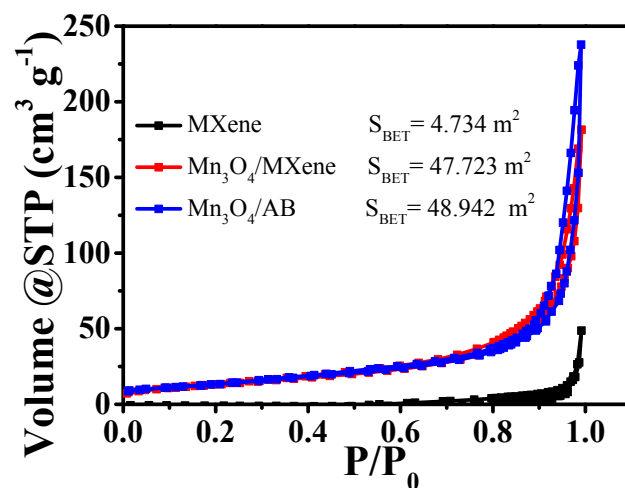


Fig. S12 Nitrogen adsorption-desorption isotherms of MXene, $\text{Mn}_3\text{O}_4/\text{MXene}$, and $\text{Mn}_3\text{O}_4/\text{AB}$. Inset is the specific surface areas of corresponding samples.

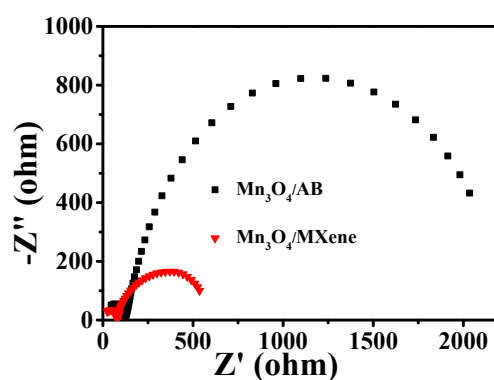


Fig. S13 Electrochemical impedance spectroscopy (EIS) spectrum of $\text{Mn}_3\text{O}_4/\text{MXene}$ and $\text{Mn}_3\text{O}_4/\text{AB}$ sample in 0.1 M KOH. Data were collected for the electrodes at -0.3 V (vs. Ag/AgCl) ranging from 1 Hz to 1 MHz.

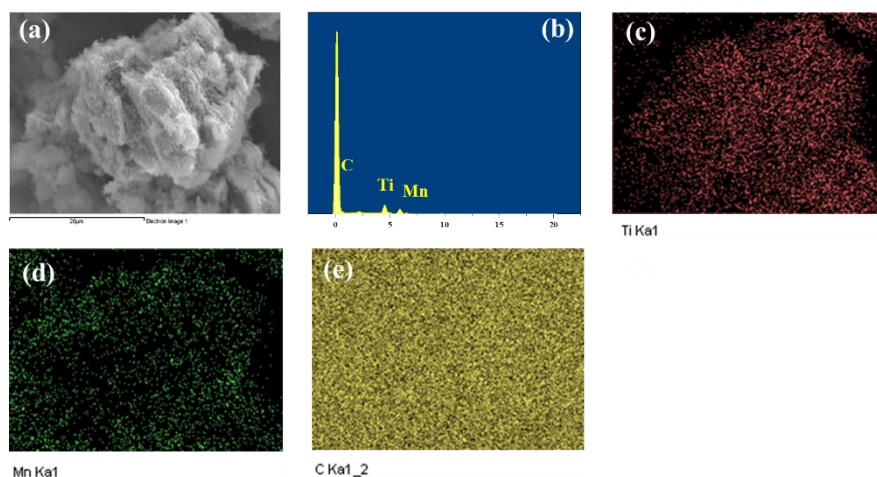


Fig. S14 (a) SEM image of Mn₃O₄/MXene after 40 h-stability test. (b) Element composition of Mn₃O₄/MXene after 40 hour-stability test. (c) Element mapping images of Ti. (d) Element mapping images of Mn. (e) Element mapping images of C.

After long-term stability test, the Mn₃O₄/MXene sample still retains the main layered structure.

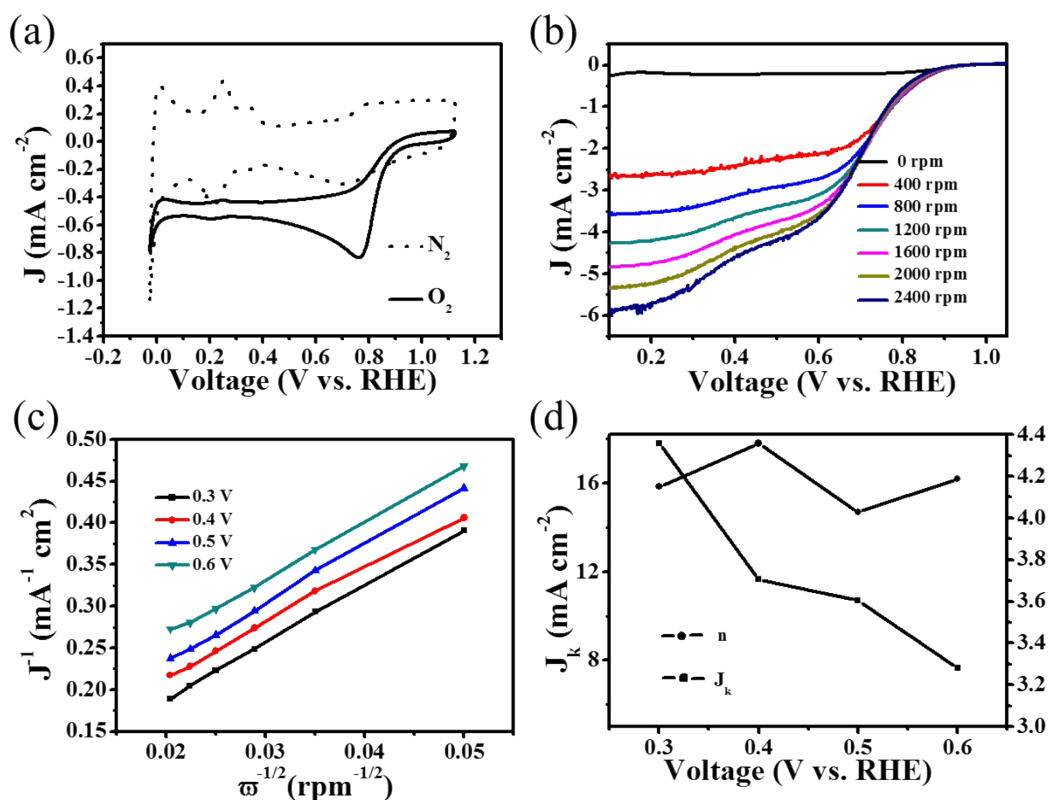


Fig. S15 (a) CV curves of Pt/C in O₂-saturated and N₂-saturated 0.1 M KOH solution (b) LSV curves of Pt/C at different rotating speed with a sweep rate of 5 mV/s. (c) Calculated K-L plots of Pt/C. (d) n - J_k curve. Catalyst loading was 0.1 mg cm².

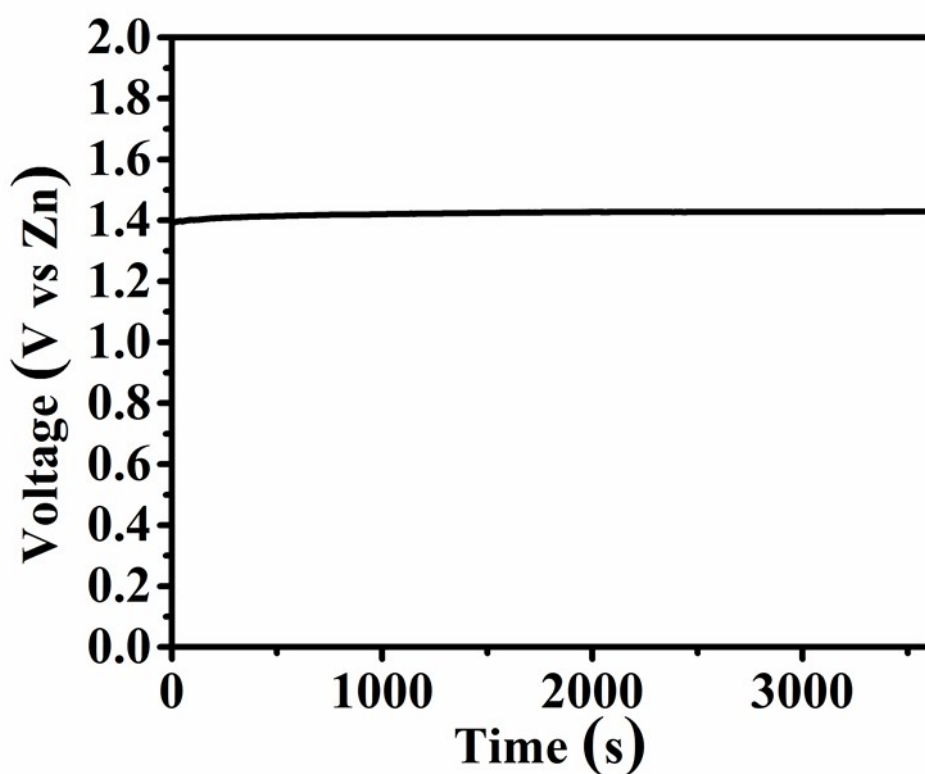


Fig. S16 Open potential of as-prepared zinc-air battery in an hour.

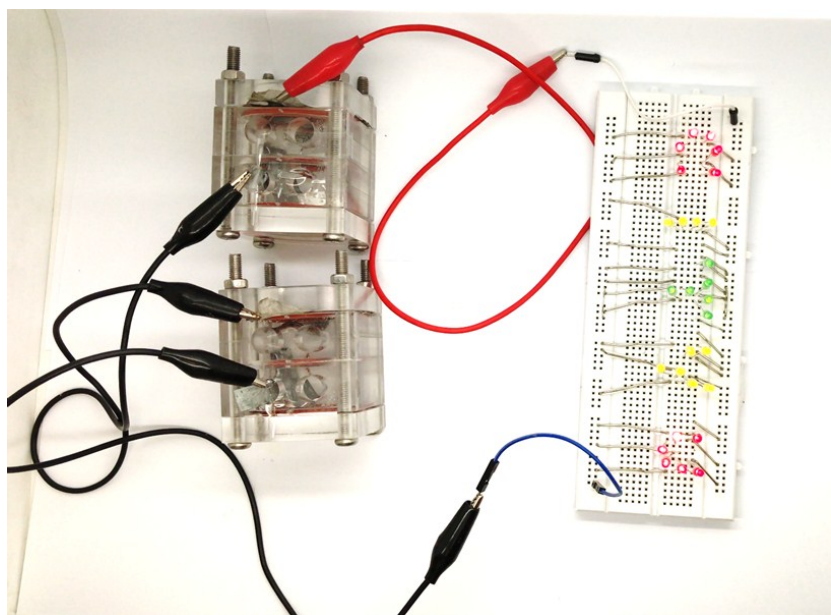


Fig. S17 Picture of connected zinc-air batteries powering a series of LEDs.

1. Duan, J. J.; Chen, S.; Dai, S.; Qiao, S. Z., *Adv. Funct. Mater.* **2014**, *24*, 2072.
2. Naguib, M.; Mashtalir, O.; Lukatskaya, M. R.; Dyatkin, B.; Zhang, C.; Presser, V.; Gogotsi, Y.; Barsoum, M. W., *Chem. Commun.* **2014**, *50*, 7420.